Risk-based path planning for autonomous underwater vehicles in an oil spill environment

Xi Chen[a, *], Neil Bose[a], Mario Brito[b], Faisal Khan[c], Gina Millar[d], Craig Bulger[e], Ting Zou[a]

[a]*Faculty of Engineering and Applied Science, Memorial University of Newfoundland, St. John's, NL A1B 3X5, Canada*

[b]*Southampton Business School, University of Southampton, University Road, Southampton SO17 1BJ, UK*

[c]*Mary Kay O'Connor Process Safety Center, Artie McFerrin Department of Chemical Engineering, Texas A&M University, College Station, College Station TX 77843-3122, USA*

[d]*Autonomous Ocean Systems Centre, Memorial University of Newfoundland, St. John's, NL A1B 3X9*

[e]*Centre for Applied Ocean Technology, Fisheries and Marine Institute of Memorial University of Newfoundland, St. John's, NL A1C 5R3, Canada*

**Corresponding author: xchen19@mun.ca*

Abstract: Autonomous underwater vehicles (AUVs) are advanced platforms for detecting and mapping oil spills in deep water. However, their applications in complex spill environments have been hindered by the risk of vehicle loss. Path planning for AUVs is an effective technique for mitigating such risks and ensuring safer routing. Yet previous studies did not address path searching problems for AUVs based on probabilistic risk reasoning. This study aims to propose an offboard risk-based path planning approach for AUVs operating in an oil spill environment. A risk model based on the Bayesian network was developed for probabilistic reasoning of risk states given varied environmental observations. This risk model further assisted in generating a spatially-distributed risk map covering a potential mission area. An A*-based searching algorithm was then employed to plan an optimal-risk path through the constructed risk map. The proposed planner was applied in a case study with a Slocum G1 Glider in a real-world spill environment around Baffin Bay. Simulation results proved that the optimal-risk planner outperforms in risk mitigation while achieving competitive path lengths

and mission efficiency. The proposed method is not constrained to AUVs but can be adapted to other marine robotic systems.

Keywords: Autonomous underwater vehicles (AUVs); probabilistic risk model; global path planning; A* algorithm; oil spill environment.

1 Introduction

An oil spill is one of the major accidents in the ocean that can damage the marine ecosystem, social economy, and human health (Hwang et al., 2020; Zhu et al., 2021). Due to hazardous effects of oil spills, it is essential to detect and track the oil during or after a spill for environmental impact assessment and response decision-making (White et al., 2016). Although surface oil slicks can be detected and mapped by traditional survey methods (i.e., satellite imagery and ship-based sampling), subsurface oil detection could be more challenging due to the deep presence of oil and its spatial-temporal changes over time (Ji et al., 2020). Autonomous underwater vehicles (AUVs) are advanced marine robots that can be used for detecting, tracking, and assessing subsurface oil in deep water (Kinsey et al., 2011; Sahoo et al., 2019). Compared with traditional survey methods, AUVs coupled with multiple sensors are superior in providing high-resolution sampling data of submerged oil plumes, achieving communication of spill information in near real-time, as well as preventing personnel exposure to hazardous oil spill environments (Pereira et al., 2013; Vinoth Kumar et al., 2020). Therefore, it is beneficial to deploy AUVs for searching and delineating subsurface oil plumes, capturing oil behaviors, and improving the efficiency of oil spill response.

Due to their ability to obtain in-situ data, some scientists have implemented AUVs for oil spill detection. During the Deepwater Horizon spill in the Gulf of Mexico, which was one of the largest oil spill accidents in history, a Sentry AUV was employed with underwater mass spectrometers to localize and track submerged oil plumes at approximately 1100 m depth (Camilli et al., 2010; Kinsey et al., 2011). A REMUS-600 AUV was deployed with a fluorometer at a natural oil seep off the coast of Santa Barbara, California, with a mission depth up to 35 m (DiPinto, 2019). A glider AUV coupled with a fluorometer was used to detect oils in Tallinn Bay in the Gulf of Finland, which proved that the glider is suitable to monitor the oil distribution over a larger sea area due to its long-endurance capability (Pärt et al., 2017). A Jaguar AUV was effectively used in the ice-mapping missions to detect the under-ice oil spills in the Northern Alaska coast (Maksym et al., 2014).

Yet none of the missions above have considered the risk of vehicle loss as part of their mission planning. However, operating in an oil spill environment could expose AUVs to the risk of loss due to the comprehensive effects of ocean currents, surface waves, potential underwater obstacles, and oil contamination on sensors. Therefore, it is essential to minimize such risks and enhance their safety navigation during spill response missions. Risk-based path planning is one of the critical techniques for mitigating risks and ensuring AUVs' safe deployment before a mission. It refers to planning an optimal path for the vehicle from its initial state to the goal state of a mission considering the risk involved, which is under certain criteria (e.g., shortest path length, minimal cruise time, minimal risk profile), and as the same time, avoiding obstacles along a path (Zeng et al., 2015; Lefebvre et al., 2016; Guo et al., 2021).

A number of studies have investigated risk-based path planning methods for AUVs to realize safer operations. Pereira et al. (Pereira et al., 2011) proposed a minimum risk planner that minimized the cumulative surfacing risk for a glider AUV. Based on this work, an expanded study (Pereira et al., 2013) considered the effects of ocean currents on the vehicle for planning AUV paths and predicted ocean currents using a probabilistic model. The proposed planner effectively reduced the collision risk with ships and land. Hegde et al. (Hegde et al., 2016) presented a method for developing collision risk indicators for AROVs. The proposed indicators (i.e., time to collision, mean time to collision, and mean impact energy) were used to identify risk prone waypoints for a given AROV path, which could further assist in mission path planning/replanning and providing risk reduction measures. Lefebvre et al. (Lefebvre et al., 2016) addressed the collision risk for AUV path planning using a hierarchical A* approach. To enhance the autonomy capability of the vehicle, the authors highlighted the integration of path planning in the AUV control architecture. However, this study only considered the underwater obstacles while ignoring other environmental information. Yan et al. (Yan et al.,

2022) applied a whale optimization algorithm to tackle a three-dimensional planning problem for AUVs. The proposed planner can effectively avoid risky regions and achieve the shortest and safest path with minimal energy consumption. Zhang et al. (Zhang et al., 2022) addressed the AUV path tracking with real-time obstacle avoidance via a reinforcement learning technique. The risk constraints were adopted in reward functions to realize collision avoidance and ensure safety control.

While previous studies have explored different risk-based path planning methods for mitigating AUV risks, limitations are observed from them. Firstly, most of the former research only addressed risks in a general marine environment with impacts of a single environmental variable, for example, the underwater currents. However, limited studies have considered the scenario of AUVs navigating in complex oil spill environments with interactions of multiple risk variables, and accordingly provided the mission planning strategy from the safety perspective. Secondly, limited past works have applied a probabilistic model for quantifying the risk state of AUVs given varied environmental observations. While probabilistic reasoning could enhance the accuracy of risk prediction and further improve the efficiency of decision making, therefore, a rigorous method that integrates a probabilistic risk model into the path planning problem for AUVs is needed.

The objective of this study is to propose a risk-based path planner for AUVs to improve its safety performance and enhance autonomous capabilities in oil spill environments. Specifically, hazardous impacts of potential risk variables in oil spill regions were analyzed. A risk analysis model based on the Bayesian network (BN) was then developed for probabilistic reasoning over current risk states of vehicle loss, which considered various environmental conditions and potential underwater obstacles. This risk model was extended to assist in generating a risk map of a gridded mission area. In order to avoid high-risky regions while achieving a relatively shorter path length, the A* algorithm was employed to search for an optimal-risk solution. The performance of the proposed planner was demonstrated in a simulated case study with a spill area in Baffin Bay.

The contribution of this study is twofold. Firstly, the proposed BN-based risk model can quantify the risk states of AUVs while assisting in intuitively presenting spatial risk distributions in the complex oil spill environment. The probabilistic reasoning can enhance the effectiveness and accuracy of further risk-based decision making. Secondly, the developed optimal-risk planner can avoid potential risky regions and obstacles, and meanwhile, it achieves a trade-off between risk mitigation and mission efficiency. It is expected that the proposed strategy can serve as a worthwhile precomputing policy to prevent AUV loss at the path planning stage, and therefore enhance the safety decision-making capability of AUVs for safer navigation. The proposed method is not constrained to AUVs but can be adapted to other marine robotic systems.

The structure of this article is organized as follows. Section 2 defines the risk-based path planning problem and the solution of this study. Section 3 elaborates a BN-based model used for risk map generation and describes the A* algorithm used for path searching. Results of a simulated case study are discussed in Section 4, and Section 5 concludes this study.

2 Risk-Based Path Planning: Problem Definition and Solution

The proposed risk-based path planner in this study aims to find an optimal-risk path based on a probabilistic risk map. In this section, the general problem formulation was defined and the solved algorithm was described.

2.1 Problem Definition

Generally, methods for AUV path planning can be broadly divided into two categories: global path planning and local path planning. Global path planning searches for a globally optimal path with known environmental information beforehand with an AUV mission, whereas local path planning finds a locally optimal strategy under unknown and dynamic environments (Cheng et al., 2021). This study mainly focused on the global path planning for AUVs, especially for a glider AUV, to plan an optimal risk path. The reason lies in that a local path planning algorithm would require an onboard implementation and consume more energy, while gliders consume low energy to secure high longevity of their missions. Therefore, real-time implementation of local path planning could be difficult considering energy consumption. In addition, environmental information for AUV missions, such as locations of large static obstacles (e.g., islands or rocks), could be obtained beforehand. In this case, it is worthwhile to conduct the offline global path planning prior to AUV missions as precomputing policies to ensure safe deployment.

In general, a global path planning problem can be formulated as an optimization problem, which can be defined as Eq. (1):

$$P^* = \underset{p_k \in P}{\operatorname{argmin}}\, g(p_k) \tag{1}$$

where $P = \{p_1, p_2, \dots, p_n\}$ is a set of feasible paths, p_k is the k^{th} path amongst the set P, and P^* denotes the optimal path that minimizes the cost function g. Through various cost functions, different optimal objectives can be realized, such as achieving the minimal involved risks, the minimal routing length, the minimal travel time, and so on.

The objective of this study is to search for an optimal-risk path for AUVs travelling from a given initial position to a goal position, whilst achieving a competitive path length. The risk state of an AUV can be specified by a risk index, which refers to the probability of vehicle loss. Hence, the objective function of this study can be modified as Eq. (2), and the cost functions of both the risk of vehicle loss and the path length are defined in Eq. (3) and Eq. (4), separately:

$$P^* = \underset{p_k \in P}{\operatorname{argmin}}[g_r(p_k) + g_l(p_k)] \tag{2}$$

$$g_r(p_k) = \sum_i r(w_i) \tag{3}$$

$$g_l(p_k) = \sum_{i-1} d(w_i, w_{i+1}) \tag{4}$$

where w_i is the i^{th} waypoint to be reached along the path p_k, $r(w_i) \in [0, 1]$ denotes the risk index of the waypoint w_i, which is calculated using the Bayes theorem as Eq. (7) that is elaborated in Section 3.1; $g_r(p_k)$ represents the accumulative risk cost along the path p_k, which is under the constraint of the risk threshold that is defined in Eq. (5); $g_l(p_k)$ represents the accumulative length cost along the path, and $d(w_i, w_{i+1})$ denotes the Euclidean distance between the two adjacent waypoints.

$$r(w_i) < r_t \tag{5}$$

where r_t is a predefined risk threshold that specifies the maximum acceptable risk index for a waypoint.

2.2 Problem Solution

To find a globally optimal-risk path, the A* algorithm was applied in this study. The A* algorithm, which is oriented from the Dijkstra's algorithm, is an effective solution for searching the globally minimum-cost path in a static network, and it is widely applied to address low-dimensional path planning problems (Dijkstra, 1959; Hart et al., 1968). The evaluation function of this algorithm is defined in Eq. (6):

$$f(w_i) = g(w_i) + h(w_i) \tag{6}$$

where $g(w_i)$ is the actual cost from the start state w_s to the current waypoint w_i in the search network, $h(w_i)$ represents the estimated cost called a heuristic from the current waypoint w_i to the goal state w_g, and $f(w_i)$ is the total cost from the start state through the waypoint w_i to the goal state.

Therefore, A* calculates the total cost $f(w_i)$ of candidate nodes in the searching network, and it selects a node with the minimal value of $f(w_i)$ as the next traversal node until reaching the goal node. Meanwhile, A* relies on a heuristic $h(w_i)$ to fast drive the network exploration to the desired areas by exploring the fewest number of nodes. This exhibits its advantage in reducing the computational time and improving the path searching efficiency (Cheng et al., 2021). Another advantage of the A* algorithm is its flexibility to be adapted by modifying the heuristic and cost functions given various optimization objectives, which is particularly beneficial to AUV path planning considering different mission requirements in complex marine environments (Singh et al., 2018). Hence, the A* algorithm has been commonly used for planning global paths of AUVs with various optimization criteria, including the shortest path length (Wang et al., 2017; Wang and Pang, 2019), the minimal collision risk (Pereira et al., 2011; Lefebvre et al., 2016), the minimal energy consumption (Li et al., 2017; Yao et al., 2018), and the shortest searching time (Szczerba et al., 2000; Li and Zhang, 2020). Given its superiority in fast searching and flexible adaptation from the risk perspective, the A* algorithm was chosen as the path planning solution in this study.

3 Methodology

The flowchart of the proposed methodology is presented in Fig. 1. It can be broadly divided into three steps. A risk analysis model based on the BN was firstly established for probabilistic reasoning of waypoint risk indices. A risk map was then created based on the BN inference results. Through the generated risk map, an A*-based algorithm was employed to search for an optimal-risk path in the potential mission area. Details of the proposed approach were elaborated in the following subsections.

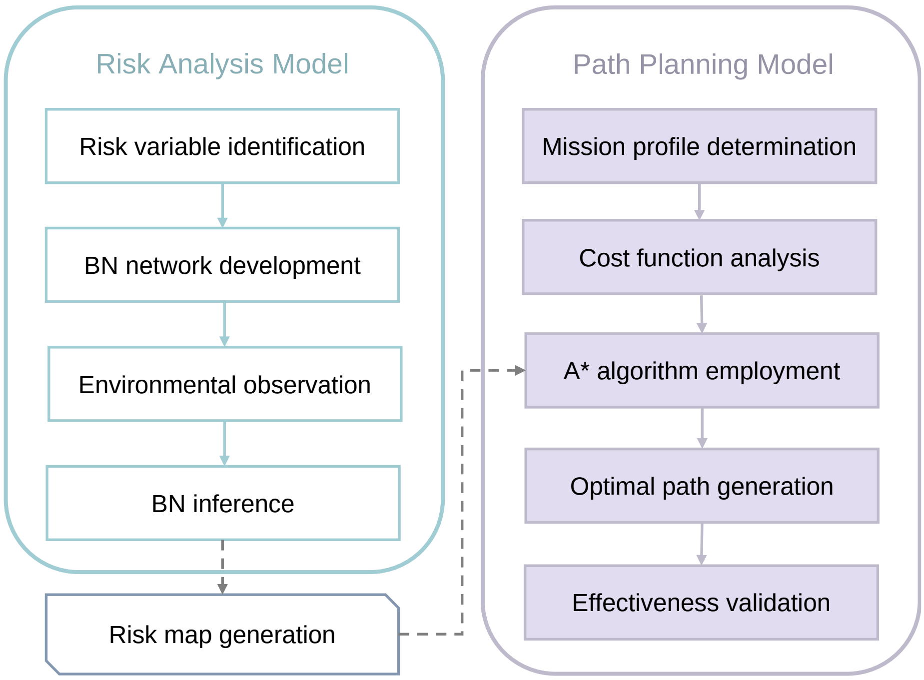

Fig. 1. Flowchart of the proposed method.

3.1 Development of a BN-based risk model

Risk variable identification is a premise to establish a BN-based risk model. Risk variables, which can potentially lead to AUV loss in an oil spill environment, should be firstly captured in this study. To facilitate further BN inference, identified risk variables can be discretized into three states according to their observed values, representing low, medium, and high severity, respectively.

BN is a probabilistic graphical model composed of vertices (nodes) and edges (arrows), where each node denotes a random variable and arrows represent causal relationships among nodes (Afenyo et al., 2017). Their dependency degrees can be captured mathematically using conditional probabilities with the Bayesian theorem. For each BN, there is a unique probability model. Assuming that X is a set of random variables: $X = (x_1, x_2, \dots, x_n)$, where n is the number of variables in the network. The joint probability $P(x_1, x_2, \dots, x_n)$ can be calculated according to the chain rule of the Bayes theorem using Eq. (7):

$$P(x_1, x_2, \dots, x_n) = \prod_{i=1}^{n} P(x_i|Pa(x_i)) \tag{7}$$

where $Pa(x_i)$ represents the set of parent nodes of x_i, and $P(x_i|Pa(x_i))$ is the conditional probability distribution.

Bayesian networks have been well applied for risk analyses in the AUV domain. Griffiths and Brito (Griffiths and Brito, 2008) firstly used a BN model for predicting the risk of AUV loss in a sea ice environment. An extended study based on it applied a BN model for AUV risk management in Polar regions (Brito and Griffiths, 2016). The proposed BN structure coped well with the uncertainties by eliciting expert judgement. Meanwhile, it captured the risk variables from both environmental factors (i.e., ice concentration, ice thickness) and the vehicle platform to produce an updated probability of vehicle loss. Hegde et al. (Hegde et al., 2018) presented a BN model for monitoring the mission abort during AUV operations of inspection, maintenance, and repair (IMR). This application of the BN model identified risk factors from technical, organizational, and operational perspectives, and it quantified the probability of the IMR mission failure. More recently, Bremnes et al. (Bremnes et al., 2019; Bremnes et al., 2020) proposed a Bayesian approach towards supervisory risk control of AUVs for under-ice operations. The BN reasoning was employed to predict the risk state for online risk modelling. The constructed risk model further assisted in decision-making for waypoint selections of the vehicle. Yang et al. (Yang et al., 2020) provided an approach for dynamic risk analyses of a long-range AUV based on a dynamic BN model. The risk state can be updated online when the vehicle experiences different operating environments, which automatically guides the AUV to avoid hazardous environmental conditions.

There are clear advantages of using the BN for AUV risk modelling. Firstly, due to complex operational environments of AUVs, multiple risk factors could interact and cause vehicle loss. While BN contains a clear topological structure to present causal relationships among complex risk variables, which facilities risk identification especially for a multi-variable system (Obeng et al., 2022). Secondly, BN is a probabilistic risk assessment tool, and using the conditional probability theory could enhance the accuracy of risk prediction. In addition, based on its predictive reasoning, BN can update the current risk state of the vehicle given new environmental observations (Yazdi et al., 2021). This feature is particularly beneficial for an AUV platform which exposes to various operating environments during a mission, and thereby its spatial-temporal evolution of risk states can be predicted timely. Lastly, BN can be easily employed by combining expertise even when the historical data are limited (Brito et al., 2022). To our knowledge, the BN model has not been used for AUV path planning. Given its superiority, this study extended the application of the BN model to the domain of AUV decision making.

3.2 Risk Map Generation

A risk map of a potential mission area can be generated based on BN reasoning results. The created risk map is represented in the form of probabilistic occupancy grids. Each grid evaluates the risk index $r(w_i) \in [0, 1]$, which is specified by the probability of the AUV loss given contained environmental conditions. As described in Section 2.1, the risk index $r(w_i)$ is calculated using the Bayes theorem as Eq. (7). Therefore, the risk map serves as a probabilistic measure of spatial risk states in the desired mission area. A trade-off should be considered when determining the grid resolution, as a relatively lower resolution could speed up the search progress but meanwhile sacrifice the accuracy of the planned vehicle's positions.

3.3 Development of the Path Planning Model

Based on the constructed risk map, an A*-based path planning model can be then applied to obtain an optimal solution from the safety perspective. It firstly analyzes the cost functions of both risk indices and path lengths. Then, the objective function can be determined according to involved costs, and the A* algorithm is finally used to search for an optimal-risk path.

3.3.1 Cost function analysis

When considering the risk cost along a path, an actual risk cost $g_r(w_i)$ of the current waypoint w_i, which was originally defined in Eq. (3), can be adapted to Eq. (8). Moreover, an admissible heuristic $h_r(w_i)$ (i.e., an estimated risk cost) used for A* searching can be defined in Eq. (9), which was adapted from former research (Pereira et al., 2011; Pereira et al., 2013; Lefebvre et al., 2016).

$$g_r(w_i) = r(w_i) \tag{8}$$

$$h_r(w_i) = N * r_{min} \tag{9}$$

where $r(w_i)$ denotes the risk index of the waypoint w_i, which was elaborated in Section 2.1. r_{min} is the globally minimum risk index among all grids in the risk map, and N is the minimal number of transitions from the current waypoint w_i to the goal w_g, which can be defined in Eq. (10):

$$N = \left\lfloor \frac{d\left(w_i, w_g\right)}{d_{max}} \right\rfloor \tag{10}$$

where $d\left(w_i, w_g\right)$ denotes the Euclidean distance between the current waypoint w_i and the goal w_g, and d_{max} is the maximum Euclidean distance between two adjacent waypoints.

When considering the length cost along a path, an actual length cost of the current waypoint $g_l(w_i)$, which was based on Eq. (4), can be adapted to Eq. (11). This actual length cost calculates the Euclidean distance $d(w_s, w_i)$ from the start point w_s to the current point w_i. We adopted an admissible heuristic $h_l(w_i)$ defined in Eq. (12), which estimates the Euclidean distance $d(w_i, w_g)$ from the current waypoint w_i to the destination w_g.

$$g_l(w_i) = d(w_s, w_i) \tag{11}$$

$$h_l(w_i) = d(w_i, w_g) \tag{12}$$

3.3.2 Objective function analysis

Based on Section 2.2, the objective function of this study combines the accumulative costs of both involved risks $f_r(w_i)$ and path lengths $f_l(w_i)$ along a path. Specifically, the risk cost $f_r(w_i)$ sums up the actual risk cost $g_r(w_i)$ and the heuristic risk cost $h_r(w_i)$. While the length cost $f_l(w_i)$ combines the actual length cost $g_l(w_i)$ and the heuristic length cost $h_l(w_i)$. Therefore, the objective function of the proposed optimal-risk planner can be specified in Eq. (13):

$$\begin{aligned} P^* = {} & \operatorname{argmin} \sum_i [f_r(w_i) + f_l(w_i)] \\ = {} & \operatorname{argmin} \sum_i \{[g_r(w_i) + h_r(w_i)] + [g_l(w_i) + h_l(w_i)]\} \end{aligned} \tag{13}$$

4 Case Study

In this section, a simulated case study using a Slocum G1 Glider was performed in a real-world oil spill environment near Baffin Bay to validate the effectiveness of the proposed path planner. Firstly, the BN model was developed by incorporating various risk variables of a spill environment. A probabilistic risk map for vehicle loss was generated, presenting the spatial risk distributions in a selected mission area. Then, the searching A* algorithm was implemented to find an optimal-risk path based on the risk map. Comparative analyses with the other two classic planners were conducted to demonstrate the superiority of the proposed optimal-risk planner.

The employed AUV type in this study is Slocum G1 Glider. Its basic specification is summarized in Table 1. Although the actual motion of a glider AUV is in three dimensions, this case study only considered a two-dimensional trajectory of the vehicle in the horizontal plane for global path planning, which is particularly relevant in missions detecting an oil spill released by vessels without consideration of significant depth changes. However, this study can be expanded to a higher dimension by considering various mission depths, and the application scenario could be monitoring oil spills from reservoirs where the vehicle is required to dive much more deeply.

Table 1. The specification of a Slocum G1 Glider (Wang et al., 2021).

Parameter	Value
Weight in Air	~52 Kg
Hull Diameter	0.213 m
Width including Wings	1.003 m
Vehicle Length	1.5 m
Minimum Turning Radius	~17 m
Displacement	52 L
Depth Range	4-200 m
Speed	0.4 m/s horizontal
Range	1500 km

4.1 Mission Profile Description

The mission area in this case study was selected as an open water area around Scott Inlet (71.10941 N, -71.10576 W), which is on the east coast of Baffin Island where oil seeps are naturally present. The satellite radar imagery has confirmed that large oil slicks over this region exceed 250 km^2, each representing over 50,000 barrels of surface oil (Oakey et al., 2012). Hence, with sufficient oil in the water, this region was chosen as a potential mission area. However, due to limited data for this area, we used information of oil concentrations in the region from a study following a hypothetical spill from an anthropogenic source. The size of the selected mission area was relatively small and set as 500 m × 500 m. The whole search space was discretized into grids and the resolution for each grid was 10 m × 10 m, namely, the minimum distance between two adjacent waypoints was 10 m. Fig. 2 illustrated the gridded mission area, where the start position and goal position were defined as (50 m, 20 m) and (450 m, 480 m) respectively in coordinates.

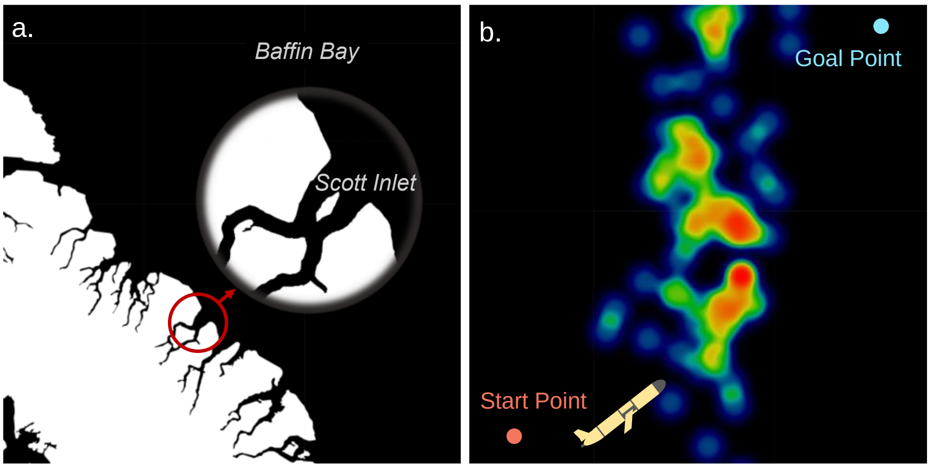

Fig. 2. Illustration of the selected mission area, where (a) shows the mission location near Scott Inlet, Baffin Bay, and (b) shows an example of a gridded spill area with the start and goal positions.

4.2 Risk Variable Identification

As a precondition for the development of the BN model, in this study, we mainly identified two types of risk variables that can lead to vehicle loss: environmental variables and mission complexity factors. In particular, we considered environmental variables including the current speed, wave height, ship density, and oil concentration. While mission complexity factors contain the mission depth and obstacle numbers. The description of identified BN variables is summarized in Table 2.

Table 2. Description and value ranges of the BN variables.

BN Variables	Description	Value Range		
		Low	Medium	High
E1	Current speed (m/s)	<0.05	0.05-0.15	>0.15
E2	Wave height (m)	<0.25	0.25-0.5	>0.5
E3	Oil concentration (ppb)	<50	50-100	>100
E4	Ship density (routes/0.08km²/year)	<20	20-50	>50
M1	Mission depth (m)	<50	50-100	>100
M2	Obstacles	/	/	/
T	AUV loss	/	/	/

4.2.1 Environmental variables

A current speed can influence the motion of an AUV by deviating it from its planned path (Griffiths and Trembanis, 2007; Petillo and Schmidt, 2012). Such impacts could be more prominent for slow-moving AUVs, such as underwater gliders. In this case, the vehicle may not reach its target position, and as a result, it could collide with other vehicles or even get lost. Surface waves could cause the vehicle out of sight, and this may lead to difficulties especially for the recovery phase of an AUV mission. In addition, the wave-induced force can also drag the vehicle from its desired path. Oil in high concentration could cause contamination of optical sensors, and substantially degrade the sensor’s ability to detect obstacles (Chen et al., 1987). In addition, if the oil coats the inside of a CTD sensor, it can possibly affect the sensor’s calibration and thus cause false measurement. Ship density is another key factor and the probability of collision between ships and AUVs is proportional to the shipping density in a mission area (Merckelbach, 2013).

4.2.2 Mission complexity factors

The number of underwater obstacles and the mission depth can influence the mission complexity. A large number of obstacles could cause higher requirements for the AUV’s ability of obstacle avoidance, and they could also raise the possibility of collisions. The mission depth can affect both the vehicle’s integrity, buoyancy control, and energy consumption (Chen et al., 2021).

4.2.3 Data sources of risk variables

In this study, environmental data in the mission area were collected based on the website of National Oceanic and Atmospheric Administration (https://www.ncei.noaa.gov/) and Marine Traffic (https://www.marinetraffic.com/). The oil concentration data used in the case study was randomly generated and referred from former research (Reich et al., 2016). Based on the above information, the collected environmental information can be visualized in Fig. 3, which presents the spatial distributions of the value of various risk variables. It should be noted that all the risk variables, except underwater obstacles, were assigned three discrete levels: low, medium, and high states, representing their severity. The expert elicitation method is a useful method to deal with limited historical data. In this study, we invited six domain experts to constitute the expert panel. The panel has sufficient experience in both the fields of AUV operations and risk assessment. The panel provided analyses and reviews including the identification of the risk variables, division of value ranges of the risk variables, assignment of prior probabilities and construction of the conditional probability tables (CPTs) for the proposed BN model. The elaborate descriptions for the expert elicitation method can be found in previous studies (Brito and Griffiths, 2016; Huang et al., 2020; Wang et al., 2022), while the detailed process of applying this method is outside the scope of the current study. The value ranges were divided in Table 2 based on the judgements of domain experts, considering the specification of the Slocum G1 Glider. The mission depth in this study was assumed as 50 m, which is at the low level according to its severity division. According to Fig. 3 (d), the severity of ship density in the selected mission area was also indicated as a low level. Fig. 3 (e) presented 200 obstacles in the mapped area which were plotted in black. The obstacles inside the mission area were randomly generated to test the capability of obstacle avoidance of the proposed planner. For simplicity, only stationary obstacles (e.g., islands, buoys, rocks, and so on) were considered. Hence, the spatial distributions of severity states for the remaining three risk variables, namely, the current speed, wave height, and oil concentration, can be simplified according to the discretized value ranges in Table 2, which can be plotted in Fig. 4.

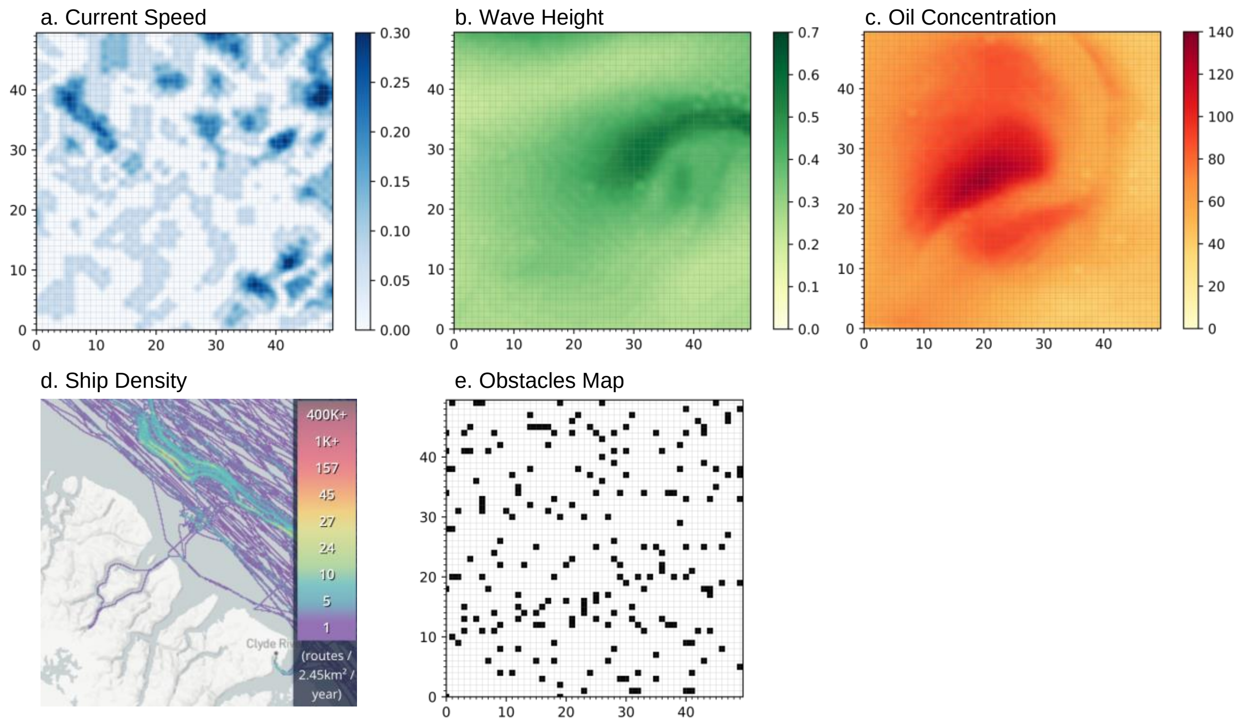

Fig. 3. Spatial data distributions of different risk variables in the selected mission area.

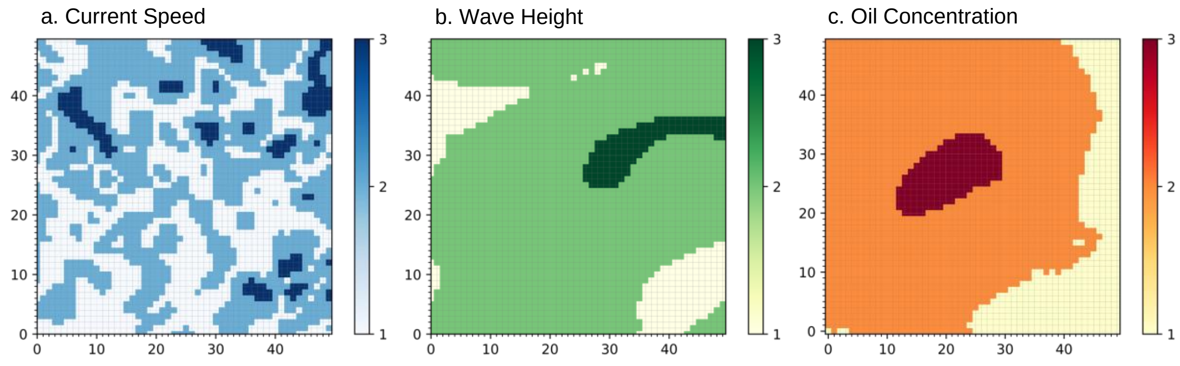

Fig. 4. Spatial distributions of severity states for the (a) current speed, (b) wave height, and (c) oil concentration.

4.3 BN Development and Risk Map Generation

Based on the above identification of potential risk variables and their causal relationships with vehicle loss, a BN model can be developed as shown in Fig. 5. The prior probability of each state of the risk variable and conditional probabilities among risk variables were determined according to domain experts' judgements.

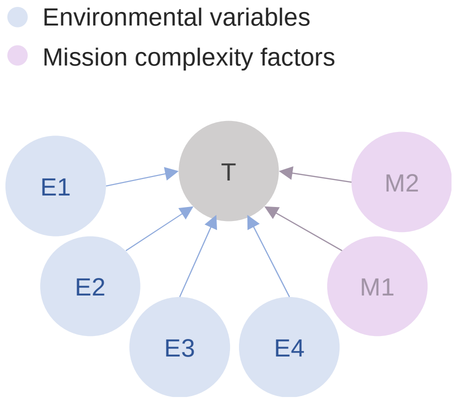

Fig. 5. Developed BN model.

On the basis of obtained environmental information and BN reasoning results, a risk map in terms of the probability of vehicle loss in the mission area can be generated and illustrated in Fig. 6. This risk map intuitively presents high-risky regions where the AUV should avoid, where the numbers on the scale represent risk indices. For instance, locations with obstacles have the highest risk index, which can always prevent the vehicle from selecting an obstacle as a waypoint. Other locations, for example, with large wave heights or with high oil concentration, also show relatively high risky in the risk map.

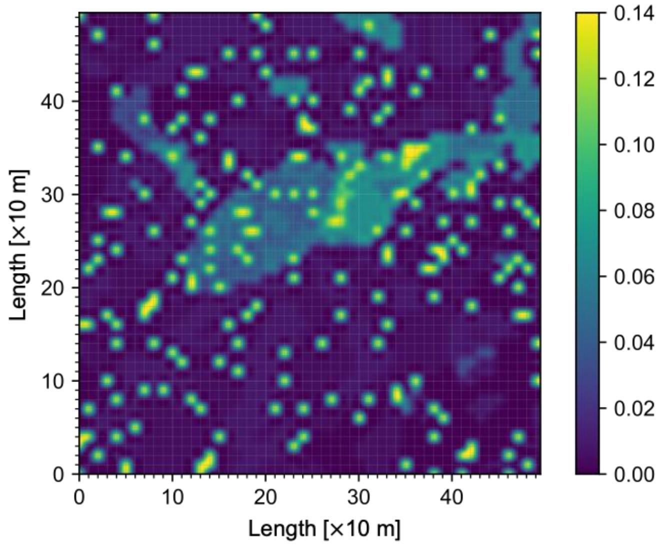

Fig. 6. Generated risk map in the mission area, where the numbers on the scale represent risk indices.

4.4 Simulation Results and Discussion

Based on the obtained risk map, an A* algorithm was employed for path planning. Effectiveness of the proposed optimal-risk planner was demonstrated by comparing it with the other two classic path planners: the minimal-length planner and the minimal-risk planner. Furthermore, influences of different risk thresholds on the optimal-risk planner were investigated. In realistic AUV operations, an acceptable risk threshold should be defined by stakeholders beforehand to a mission. While in this study, the risk threshold was defined by the expert panel to forbid the vehicle from selecting a waypoint with an unacceptable risk index. According to Fig. 6, the maximum risk index (i.e., the probability of vehicle loss) in the mission area is 0.14. A relatively low threshold of 0.05, which is around 36% of the maximum risk index, was used to rigorously test the vehicle's ability of avoiding risky regions. It is noted that the predefined risk threshold can be tuned according to the willingness of risk tolerance. While the specific method for determining the risk threshed is not within the scope of this study.

4.4.1 Comparative analyses of the three path planners

We conducted simulations using the three path planners (i.e., minimal-length planner, minimal-risk planner, and the proposed optimal-risk planner) in the same risk map. The obtained paths were presented in Fig. 7 (left column), while their waypoint risk indices and accumulative risk indices along the path were compared in Fig. 7 (right column). The start and goal positions were arbitrarily set and depicted with red and blue dots, respectively. Searched paths of the three planners show obvious differences while only the minimal-risk planner and optimal-risk planner can successfully avoid obstacles. In Fig. 7 (a), the minimal-length planner finds the shortest path from the start position to the destination without considering the cost of waypoint risks. Hence, its obtained path is approximately straight and directly toward the target. But with this said, a number of waypoints' risk indices along this path far exceed the predefined risk threshold of 0.05. For instance, the peak value (0.1) of the waypoint risk index occurs at the mission distance of 140 m, where the vehicle is directly passing through a high-risky area as shown in the risk map. On the contrary, Fig. 7 (b) shows that the minimal-risk path selects a set of waypoints with the lowest risk index, no matter how much path lengths cost. The resulted path is long and winding, which loiters to avoid any potential risky regions rather than making progress toward the goal. While the proposed optimal-risk planner, as shown in Fig. 7 (c), considers the costs of both the path length and waypoint risks. It searches a path with a moderate risk level and relatively shorter mission distance, and meanwhile, it satisfies the constraint of the risk threshold at each waypoint.

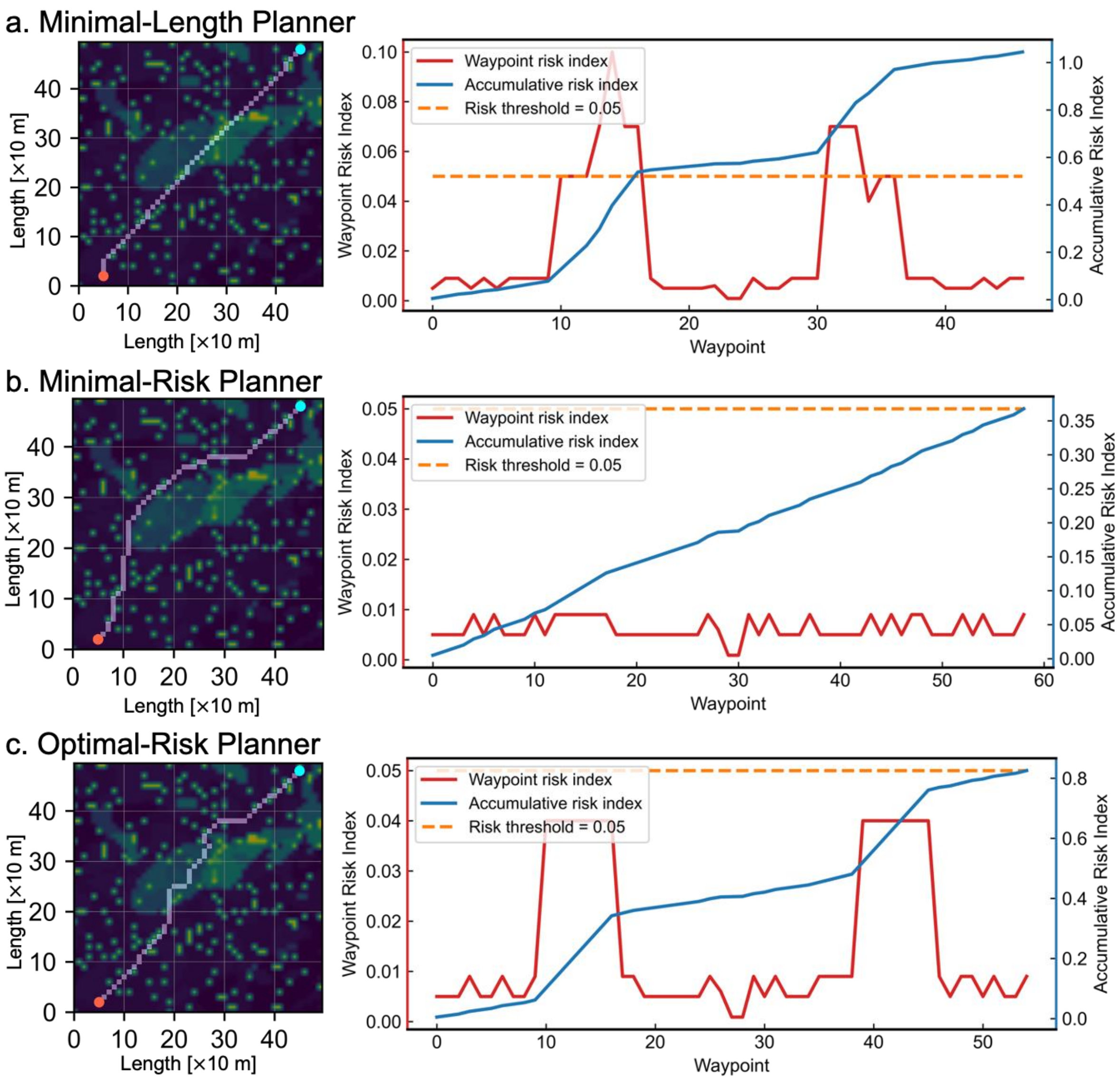

Fig. 7. Obtained paths, waypoint risk indices, and accumulative risk indices of the three path planners: (a) minimal-length planner; (b) minimal-risk planner; and (c) optimal-risk planner.

To provide additional comparisons, Fig. 8 compares the path length, max risk index (i.e., the maximum of waypoint risk indices), accumulative risk index, and computational time of three planners, respectively. The computational time of the three planners was normalized for comparison. The reference time, which was defined as 100%, was chosen as the computational time of the minimal-risk planner. Although this study mainly explored an offline global path planning approach for AUVs prior to a mission, computational time is still a key parameter to be considered. It impacts the efficiency of mission planning, which is important especially in dealing with large-scale planning problems with complex environmental conditions and long mission endurance. It can be seen from Fig. 8 (a) and (b) that the minimal-path length achieves the shortest path length of 627 m, however, its max risk index far exceeds the predefined risk threshold of 0.05, which is not acceptable for the safety requirement. On the contrary, the minimal-risk planner has the minimal max risk index among the three planners, which is only 0.009. In return, it has the largest path length, which is 12.6% higher compared with the minimal-length planner. As for the optimal-risk planner, its max risk index is 20% lower than the risk threshold (0.05), which means risk states along the whole path remain tolerable. In addition, its path length is 10.2% longer than the minimal-length planner. As it aims to mitigate risks associated with the path to ensure safe deployment, although it could sacrifice certain mission lengths.

In comparing the accumulated risk index in Fig. 8 (c), it is noteworthy that the minimal-length planner attains the largest value of 1.04, which is nearly triple that of the minimal-risk planner (0.37). However, the minimal-risk planner achieves the minimum accumulative risks at the expense of routing length, and in turn, the searching time could substantially increase along with an increasing number of waypoints. In this case, the computational time of the minimal-risk planner in finding a solution could also grow correspondingly, which reaches the maximum amongst these three planners, as shown in Fig. 8 (d). In contrast, the proposed optimal-risk planner performs moderately well, namely, its accumulative risk index is decreased by 20.2% compared with the minimal-length planner, whilst its computational time is 9.5% shorter than the minimal-risk planner.

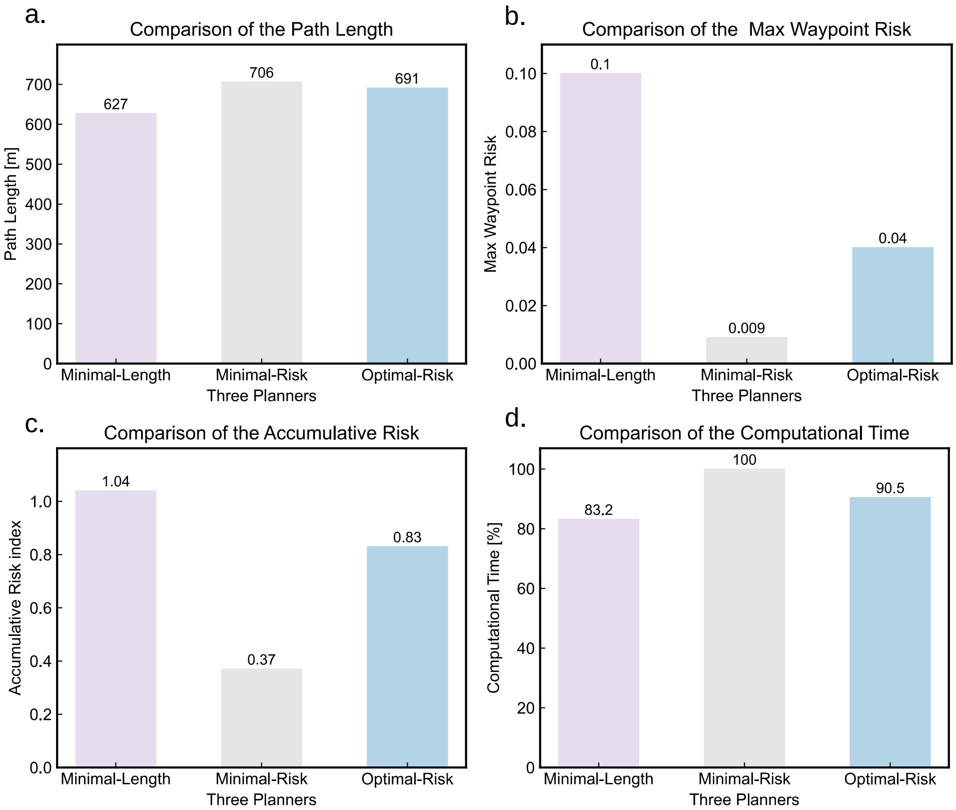

Fig. 8. Comparisons of the three planners including (a) path length, (b) max waypoint risk index, (c) accumulative risk index, and (d) normalized computational time.

Based on the above analyses, it can be concluded that: (1) The minimal-length planner outperforms in both the routing length and computational time. However, it overlooks the risk associated with the path, and as a result, the waypoint risk index exceeds a predefined risk threshold, which is unacceptable in terms of the vehicle's safety requirement in real implementation. (2) The minimal-risk path is clearly over-conservative. Although it has the lowest waypoint risk index, it comes at a cost of the path distance, which further leads to the increasing computational time. Such a path could be infeasible in practice as it might fail to meet the criteria of available energy consumption for the vehicle. (3) The optimal-risk planner is a safer bet that exhibits good performance in avoiding risky regions along a path. It also achieves a balance between the involved risks, the path length, and computational efficiency. At the same time, it satisfies the precondition of operating below a risk tolerance threshold to ensure safe navigation.

4.4.2 Influences of different risk thresholds on the optimal-risk planner

Determination of a risk threshold is also an important issue for planning an AUV route. Impacts of various risk thresholds on the proposed optimal-risk planner were investigated. Fig. 9 plots the resulting paths under four different risk thresholds in the same environment. When the tolerable risk threshold gradually decreases, which refers to a higher safety requirement for the vehicle that demands more rigorous risk tolerance, the resulting path gets longer and the AUV moves further away from potential high-risky regions to attain the acceptable risk level, which consequently wastes additional route lengths.

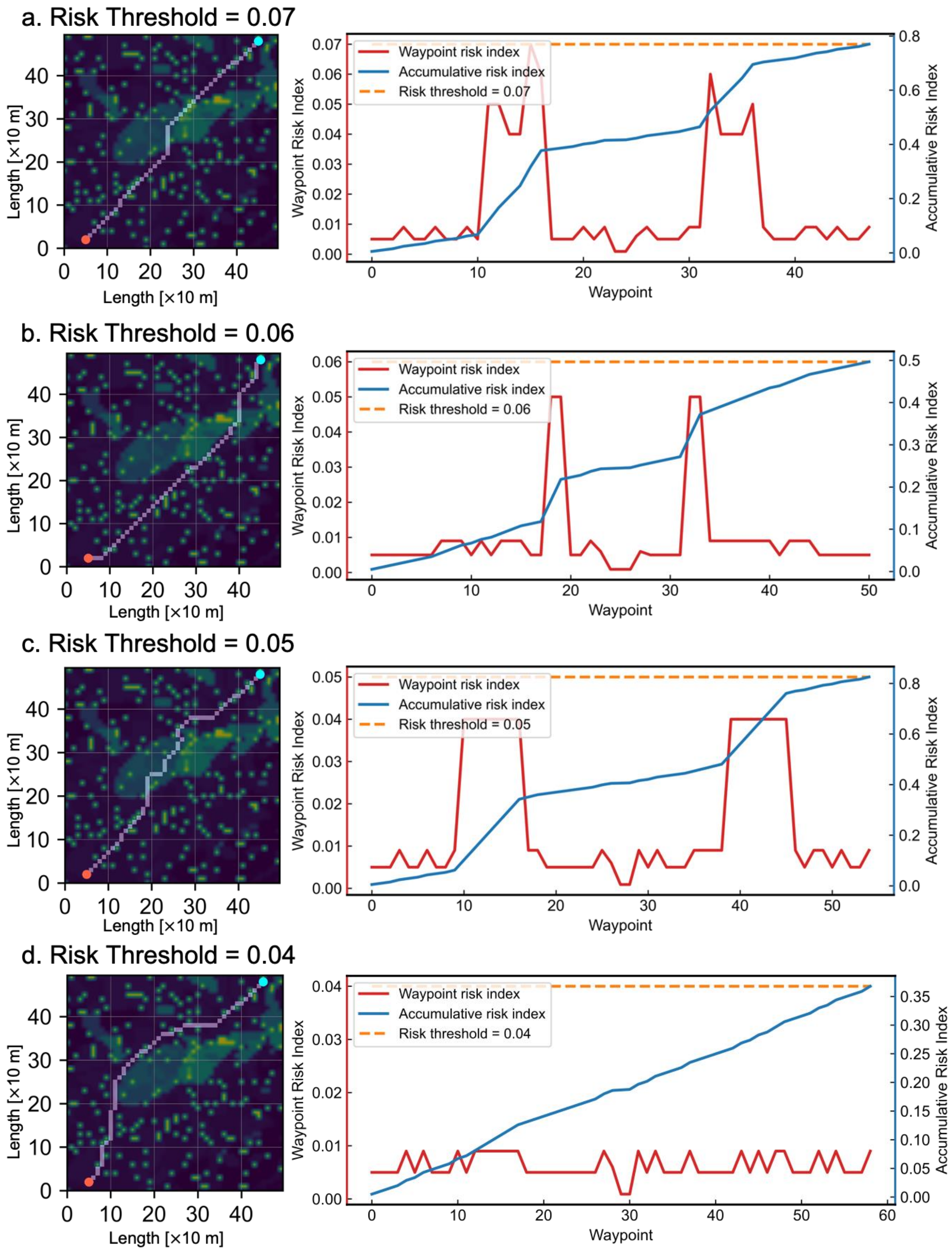

Fig. 9. Obtained paths, waypoint risk indices, and accumulative risk indices under different risk thresholds.

Particularly, Fig. 10 compares the path length, max risk index, accumulative risk index, and the normalized computational time under four risk thresholds. As shown in Fig. 10 (a), with decreasing risk threshold from 0.07 to 0.04, the path length increases from 650 m to 706 m with a changing rate of 8.6%. This implies that it is possible to achieve a higher safety level with a reduced risk threshold while only slightly degrading its length optimality. Similarly, the computational time in Fig. 10 (d) shows the same trend, which consumes 7.6% longer time when the risk threshold reduces from 0.07 to 0.04. In Fig. 10 (b), the max waypoint risk index drops gradually with the decreasing risk thresholds. It is noteworthy in Fig. 10 (c) that the accumulative risk index under the risk threshold of 0.05 is higher than that under the risk threshold of 0.06. This manifests a particular situation that should be considered in realistic mission planning, as a path with a lower risk tolerance could require more path lengths to avoid risky regions, and in turn, the accumulative risks could substantially increase along with the increasing traversed waypoints.

Therefore, the safest path does not indicate an optimal solution in practice, because it may sacrifice the mission length and deteriorate the computational efficiency at the same time. This prompts an insight to adjust the risk threshold for achieving a trade-off between an acceptable risk tolerance and the mission efficiency.

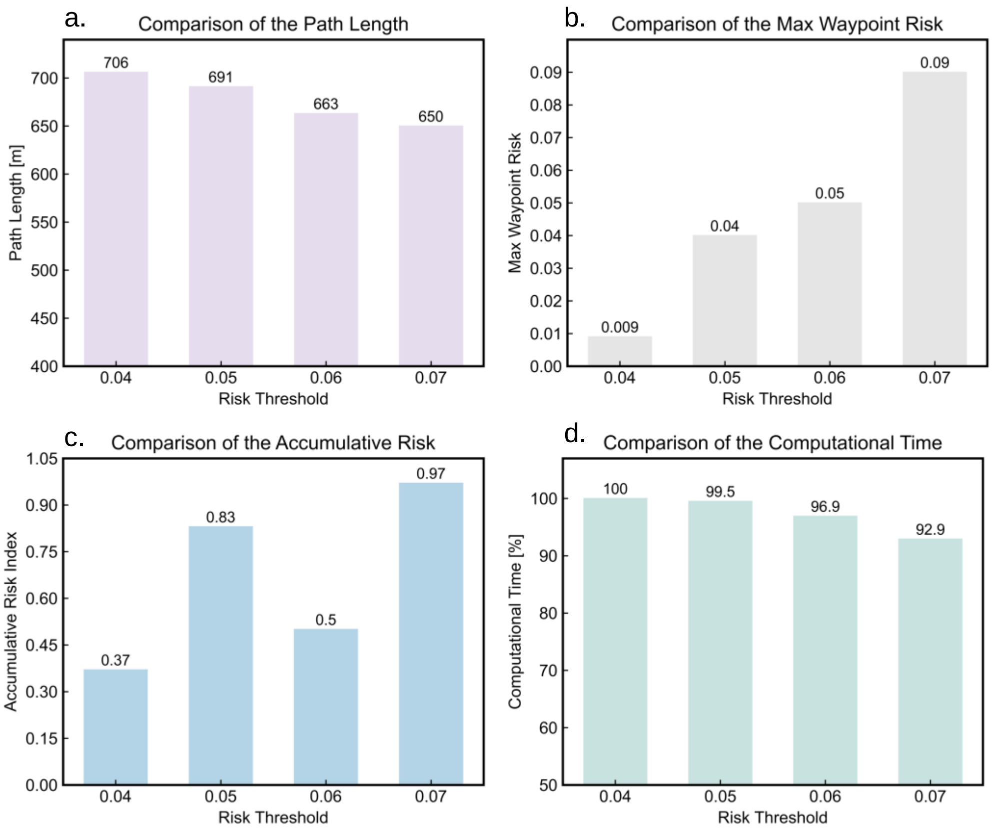

Fig. 10. Comparisons under different risk thresholds including (a) path length, (b) max waypoint risk index, (c) accumulative risk index, and (d) normalized computational time.

4.5 Limitations and Future Work

Limitations of this study were discussed below. This work only considered static environmental conditions and obstacles for global path planning of AUVs. It is desirable to conduct such offline mission planning beforehand given known environmental information. However, static global path planning requires accurate environmental predictions prior to a mission, which is difficult to achieve in reality, and it is possible that only limited environmental information can be obtained for a target mission area. In addition, ambient environmental conditions, such as ocean currents and oil spills themselves, can change dynamically, which subsequently causes the risk of vehicle loss to varying accordingly. The possibility of colliding with moving obstacles also exists. In such cases, global path planning designed for static environments cannot handle the unpredictable situations that may emerge, and re-planned solutions will be required to account for dynamic environmental observations. Hence, future research should explore a hybrid risk-based architecture for AUVs' autonomous mission planning to combine static global planning and dynamic local re-planning, which is essential for the real-life decision making of AUV missions. Furthermore, former research provided robust methods for model validation to bridge the gap between pure computer-based simulations and real experiment validation (Albarakati et al., 2021; Liu et al., 2022). For field trial validation, other key parameters beside the path length should be considered, such as the vehicle velocity, turning maneuvers, travel time, and energy consumption, which can be affected by ambient environmental conditions. An accurate estimation of AUVs navigational data is also crucial for safe path planning. The use of multiple sensors' data could be beneficial for high-fidelity validation in practical environments.

5 Conclusion

In this study, a systematic risk-based path planning approach for AUVs operating in an oil spill environment was proposed. The risk of vehicle loss was incorporated into a classic global planning problem of AUVs. A BN-based risk model was developed for probabilistic prediction of risk states given various environmental observations. The established risk model was then employed to generate a spatially-distributed risk map covering a potential mission area. Subsequently, an A* algorithm was applied to plan an optimal-risk path through the risk map by combining costs of mission lengths and risk indices. The proposed path planner aims to avoid high-risky regions to ensure safer operations, whilst achieving a relatively shorter path length. A case study using a Slocum G1 Glider in an oil spill environment around Baffin Bay was conducted to demonstrate the effectiveness of the proposed planner. Key findings from the case study results were highlighted below:

(1) The proposed BN-based risk model can forecast risk states of vehicle loss given comprehensive spill environments. Its probabilistic reasoning enhances the accuracy for further path searching and risk-based decision making. The generated risk map based on BN reasoning intuitively presents the spatial distributions of high-risky regions in a gridded mission area, which provides insights of risk mitigation through obstacle avoidance and waypoint selections.

(2) Comparisons between the optimal-risk planner with two classic path planners (i.e., minimal-length planner and minimal-risk planner) have indicated that a trade-off exists between the routing length, associated risks, and computational efficiency along a path. The proposed optimal-risk planner outperforms in risk mitigation by avoiding potential risky regions and obstacles, whilst it is highly competitive in terms of path distance and computational time.

(3) Different risk thresholds can affect the performance of optimal-risk path planning. A lower tolerable risk threshold, which refers to a higher safety requirement, can increase the mission length and consume more computational time. In this case, considering a particular scenario during an oil detection mission, a lower risk threshold can drag the vehicle away from the most highly-concentrated oil regions, which causes the vehicle to miss nearby plumes with

rich information and thereby degrading its detection efficiency. Hence, the risk threshold should be modulated to achieve a trade-off between safety performance and mission efficiency.

(4) The developed risk-based planner can be practical in realistic AUV implementation. Although this study only investigated the off-line global path planning for AUVs with static environmental conditions, it is a potential precomputing policy to save the computational memory for a vehicle, and it is a worthwhile investigation for preventing AUV loss at the path planning stage prior to a mission. In addition, this study considered a two-dimensional trajectory of AUVs, which is particularly useful for missions in detecting oil spills released by vessels without significant depth changes. The approach could also be applied for AUV path planning in tracking oil spills from reservoirs. For this scenario, the vehicle would have to dive to higher depths. To capture this scenario, both the risk model and the path searching algorithm should be updated to take a 3D problem into consideration. A modification would be required to our methodology to include the 3D body dynamics property of the AUV.

Future work based on this study should incorporate dynamic risks into the path planning framework for AUVs. To this end, a hybrid risk-based path planner combining both static global planning and dynamic local re-planning for AUVs should be investigated.

Acknowledgements

This study was funded by Fisheries and Oceans Canada through the "*Multi-partner Oil Spill Research Initiative (MPRI) 1.03: Oil spill reconnaissance and delineation through robotic autonomous underwater vehicle technology in open and iced waters*" and the NSERC Alliance Project "*Characterization and delineation of oil-in-water at the Scott Inlet seeps through robotic autonomous underwater vehicle technology 2021-2024*". Coauthor, Faisal Khan, wishes to acknowledge the financial support provided by the Canada Research Chair (Tier 1) program on Offshore Safety and Risk Engineering. The authors also acknowledge Memorial University and the School of Graduate Studies (SGS) for their component of fellowship support.

References

Afenyo, M., Khan, F., Veitch, B., Yang, M., 2017. Arctic shipping accident scenario analysis using Bayesian Network approach. Ocean Engineering 133, 224-230. doi:https://doi.org/10.1016/j.oceaneng.2017.02.002

Albarakati, S., Lima, R.M., Theußl, T., Hoteit, I., Knio, O., 2021. Multiobjective Risk-Aware Path Planning in Uncertain Transient Currents: An Ensemble-Based Stochastic Optimization Approach. IEEE Journal of Oceanic Engineering 46 (4), 1082-1098. doi:https://doi.org/10.1109/JOE.2021.3063196

Bremnes, J.E., Norgren, P., Sørensen, A.J., Thieme, C.A., Utne, I.B., 2019. Intelligent Risk-Based Under-Ice Altitude Control for Autonomous Underwater Vehicles, OCEANS 2019 MTS/IEEE SEATTLE. IEEE, Seattle, WA, USA, pp. 1-8.

Bremnes, J.E., Thieme, C.A., Sørensen, A.J., Utne, I.B., Norgren, P., 2020. A Bayesian approach to supervisory risk control of AUVs applied to under-ice operations. Marine Technology Society Journal 54 (4), 16-39. doi:https://doi.org/10.4031/MTSJ.54.4.5

Brito, M., Griffiths, G., 2016. A Bayesian approach for predicting risk of autonomous underwater vehicle loss during their missions. Reliability Engineering & System Safety 146, 55-67. doi:https://doi.org/10.1016/j.ress.2015.10.004.

Brito, M.P., Stevenson, M., Bravo, C., 2022. Subjective machines: Probabilistic risk assessment based on deep learning of soft information. Risk Analysis. doi:https://doi.org/10.1111/risa.13930

Camilli, R., Reddy, C.M., Yoerger, D.R., Mooy, B.A.S.V., Jakuba, M.V., Kinsey, J.C., McIntyre, C.P., Sylva, S.P., Maloney, J.V., 2010. Tracking Hydrocarbon Plume Transport and Biodegradation at Deepwater Horizon. Science 330 (6001), 201-204. doi:https://doi.org/10.1126/science.1195223

Chen, A.T., Abe, N.D., Mullen, C.R., Gilbert, C.C., 1987. Contamination Sensitivity And Control Of Optical Sensors. SPIE, pp. 97-126.

Chen, X., Bose, N., Brito, M., Khan, F., Thanyamanta, B., Zou, T., 2021. A Review of Risk Analysis Research for the Operations of Autonomous Underwater Vehicles. Reliability Engineering & System Safety 216, 108011. doi:https://doi.org/10.1016/j.ress.2021.108011

Cheng, C., Sha, Q., He, B., Li, G., 2021. Path planning and obstacle avoidance for AUV: A review. Ocean Engineering 235, 109355. doi:https://doi.org/10.1016/j.oceaneng.2021.109355

Dijkstra, E.W., 1959. A note on two problems in connexion with graphs. Numerische Mathematik 1 (1), 269-271. doi:https://doi.org/10.1007/BF01386390

DiPinto, L., 2019. Three-dimensional mapping of dissolved hydrocarbons and oil droplets using a REMUS-600 autonomous underwater vehicle. Report to Bureau of Safety and Environmental Enforcement (BSEE).

Griffiths, G., Brito, M., 2008. Predicting risk in missions under sea ice with autonomous underwater vehicles, 2008 IEEE/OES Autonomous Underwater Vehicles. IEEE, pp. 1-7.

Griffiths, G., Trembanis, A., 2007. Towards a risk management process for autonomous underwater vehicles. Masterclass in AUV technology for polar science, 103-118.

Guo, Y., Liu, H., Fan, X., Lyu, W., 2021. Research Progress of Path Planning Methods for Autonomous Underwater Vehicle. Mathematical Problems in Engineering 2021, 8847863. doi:https://doi.org/10.1155/2021/8847863

Hart, P.E., Nilsson, N.J., Raphael, B., 1968. A Formal Basis for the Heuristic Determination of Minimum Cost Paths. IEEE Transactions on Systems Science and Cybernetics 4 (2), 100-107. doi:https://10.1109/TSSC.1968.300136

Hegde, J., Utne, I.B., Schjølberg, I., 2016. Development of collision risk indicators for autonomous subsea inspection maintenance and repair. Journal of Loss Prevention in the Process Industries 44, 440-452. doi:https://doi.org/10.1016/j.jlp.2016.11.002

Hegde, J., Utne, I.B., Schjølberg, I., Thorkildsen, B., 2018. A Bayesian approach to risk modeling of autonomous subsea intervention operations. Reliability Engineering & System Safety 175, 142-159.

doi:https://doi.org/10.1016/j.ress.2018.03.019
Huang, W., Zhang, Y., Kou, X., Yin, D., Mi, R., Li, L., 2020. Railway dangerous goods transportation system risk analysis: An Interpretive Structural Modeling and Bayesian Network combining approach. Reliability Engineering & System Safety 204, 107220. doi:https://doi.org/10.1016/j.ress.2020.107220
Hwang, J., Bose, N., Nguyen, H.D., Williams, G., 2020. Acoustic Search and Detection of Oil Plumes Using an Autonomous Underwater Vehicle. Journal of Marine Science and Engineering 8 (8), 618. doi:https://doi:10.3390/jmse8080618
Ji, C., Beegle-Krause, C.J., Englehardt, J.D., 2020. Formation, Detection, and Modeling of Submerged Oil: A Review. Journal of Marine Science and Engineering 8 (9), 642. doi:https://doi:10.3390/jmse8090642
Kinsey, J.C., Yoerger, D.R., Jakuba, M.V., Camilli, R., Fisher, C.R., German, C.R., 2011. Assessing the Deepwater Horizon oil spill with the sentry autonomous underwater vehicle, 2011 IEEE/RSJ International Conference on Intelligent Robots and Systems, pp. 261-267.
Lefebvre, N., Schjølberg, I., Utne, I.B., 2016. Integration of risk in hierarchical path planning of underwater vehicles. IFAC-PapersOnLine 49 (23), 226-231. doi:https://doi.org/10.1016/j.ifacol.2016.10.347
Li, J., Kang, H., Park, G., Suh, J., 2017. Real Time Path Planning of Underwater Robots in Unknown Environment, 2017 International Conference on Control, Artificial Intelligence, Robotics & Optimization (ICCAIRO), pp. 312-318.
Li, M., Zhang, H., 2020. AUV 3D Path Planning Based On A Algorithm, 2020 Chinese Automation Congress (CAC), pp. 11-16.
Liu, W., Liu, Y., Bucknall, R., 2022. Filtering based multi-sensor data fusion algorithm for a reliable unmanned surface vehicle navigation. Journal of Marine Engineering & Technology, 1-17. doi:https://doi.org/10.1080/20464177.2022.2031558
Maksym, T., Singh, H., Bassett, C., Lavery, A., Freitag, L., Sonnichsen, F., Wilkinson, J., 2014. Oil Spill Detection and mapping under arctic sea ice using autonomous underwater vehicles. BSEE Contract E12PC00053.
Merckelbach, L., 2013. On the probability of underwater glider loss due to collision with a ship. Journal of Marine Science Technology 18 (1), 75-86. doi:https://doi.org/10.1007/s00773-012-0189-7
Oakey, G.N., Moir, P.N., Brent, T., Dickie, K., Jauer, C., Bennett, R., Williams, G., MacLean, B., Budkewitsch, P., Haggart, J., 2012. The Scott Inlet–Buchan Gulf oil seeps: actively venting petroleum systems on the northern Baffin margin offshore Nunavut, Canada, Canadian Society of Petroleum Geologists, Annual Convention, Calgary, Alberta.
Obeng, F., Domeh, V., Khan, F., Bose, N., Sanli, E., 2022. Analyzing operational risk for small fishing vessels considering crew effectiveness. Ocean Engineering 249, 110512. doi:https://doi.org/10.1016/j.oceaneng.2021.110512
Pärt, S., Kõuts, T., Vahter, K., 2017. Oil detection using oil sensors on autonomous underwater vehicles. D1.5. wp1: oil spill detection, monitoring, fate and distribution. Integrated Oil Spill Response Actions and Environmental Effects Project (GRACE).
Pereira, A.A., Binney, J., Hollinger, G.A., Sukhatme, G.S., 2013. Risk‐aware path planning for autonomous underwater vehicles using predictive ocean models. Journal of Field Robotics 30 (5), 741-762. doi:https://doi.org/10.1002/rob.21472
Pereira, A.A., Binney, J., Jones, B.H., Ragan, M., Sukhatme, G.S., 2011. Toward risk aware mission planning for Autonomous Underwater Vehicles, 2011 IEEE/RSJ International Conference on Intelligent Robots and Systems, pp. 3147-3153.
Petillo, S.M., Schmidt, H., 2012. Autonomous and adaptive underwater plume detection and tracking with AUVs: Concepts, methods, and available technology. IFAC Proceedings Volumes 45 (27), 232-237. doi:https://doi.org/10.3182/20120919-3-IT-2046.00040

Reich, D., Etkin, D., Rowe, G., Zamorski, S., 2016. Modeling oil spill trajectories in Baffin Bay and Lancaster Sound. WWF-Canada Oil Spill Modeling Report.
Sahoo, A., Dwivedy, S.K., Robi, P.S., 2019. Advancements in the field of autonomous underwater vehicle. Ocean Engineering 181, 145-160. doi:https://doi.org/10.1016/j.oceaneng.2019.04.011
Singh, Y., Sharma, S., Sutton, R., Hatton, D., Khan, A., 2018. A constrained A* approach towards optimal path planning for an unmanned surface vehicle in a maritime environment containing dynamic obstacles and ocean currents. Ocean Engineering 169, 187-201. doi:https://doi.org/10.1016/j.oceaneng.2018.09.016
Szczerba, R.J., Galkowski, P., Glicktein, I.S., Ternullo, N., 2000. Robust algorithm for real-time route planning. IEEE Transactions on Aerospace and Electronic Systems 36 (3), 869-878. doi:https://10.1109/7.869506
Vinoth Kumar, S., Jayaparvathy, R., Priyanka, B.N., 2020. Efficient path planning of AUVs for container ship oil spill detection in coastal areas. Ocean Engineering 217, 107932. doi:https://doi.org/10.1016/j.oceaneng.2020.107932
Wang, L., Pang, S., 2019. Chemical Plume Tracing using an AUV based on POMDP Source Mapping and A-star Path Planning, OCEANS 2019 MTS/IEEE SEATTLE, pp. 1-7.
Wang, W., He, X., Li, Y., Shuai, J., 2022. Risk analysis on corrosion of submarine oil and gas pipelines based on hybrid Bayesian network. Ocean Engineering 260, 111957. doi:https://doi.org/10.1016/j.oceaneng.2022.111957
Wang, Y., Bulger, C., Thanyamanta, W., Bose, N., 2021. A Backseat Control Architecture for a Slocum Glider. Journal of Marine Science and Engineering 9 (5), 532. doi:https://doi.org/10.3390/jmse9050532
Wang, Z., Xiang, X., Yang, J., Yang, S., 2017. Composite Astar and B-spline algorithm for path planning of autonomous underwater vehicle, 2017 IEEE 7th International Conference on Underwater System Technology: Theory and Applications (USYS), pp. 1-6.
White, H.K., Conmy, R.N., MacDonald, I.R., Reddy, C.M., 2016. Methods of Oil Detection in Response to the Deepwater Horizon Oil Spill. Oceanography 29 (3), 76-87.
Yan, Z., Zhang, J., Zeng, J., Tang, J., 2022. Three-dimensional path planning for autonomous underwater vehicles based on a whale optimization algorithm. Ocean Engineering 250, 111070. doi:https://doi.org/10.1016/j.oceaneng.2022.111070
Yang, R., Utne, I., Liu, Y., Paltrinieri, N., 2020. Dynamic risk analysis of operation of the autonomous underwater vehicle (auv). The 30th European Safety and Reliability Conference and the 15th Probabilistic Safety Assessment and Management.
Yao, X., Wang, F., Wang, J., Zhao, J., 2018. Time-optimal Path Planning to Solve Motion Direction Restrict with Lower Computational Cost, 2018 37th Chinese Control Conference (CCC), pp. 5245-5250.
Yazdi, M., Khan, F., Abbassi, R., 2021. Microbiologically influenced corrosion (MIC) management using Bayesian inference. Ocean Engineering 226, 108852. doi:https://doi.org/10.1016/j.oceaneng.2021.108852
Zeng, Z., Lian, L., Sammut, K., He, F., Tang, Y., Lammas, A., 2015. A survey on path planning for persistent autonomy of autonomous underwater vehicles. Ocean Engineering 110, 303-313. doi:https://doi.org/10.1016/j.oceaneng.2015.10.007
Zhang, C., Cheng, P., Du, B., Dong, B., Zhang, W., 2022. AUV path tracking with real-time obstacle avoidance via reinforcement learning under adaptive constraints. Ocean Engineering 256, 111453. doi:https://doi.org/10.1016/j.oceaneng.2022.111453
Zhu, K., Mu, L., Xia, X., 2021. An ensemble trajectory prediction model for maritime search and rescue and oil spill based on sub-grid velocity model. Ocean Engineering 236, 109513. doi:https://doi.org/10.1016/j.oceaneng.2021.109513